Carbohydrate Polymers 112 (2014) 284–290

Contents lists available at ScienceDirect

Carbohydrate Polymers

journal homepage: www.elsevier.com/locate/carbpol

Aqueous counter collision using paired water jets as a novel means of preparing bio-nanofibers

Tetsuo Kondo[a,*], Ryota Kose[b], Hiroki Naito[a], Wakako Kasai[a]

[a] Graduate School of Bioresource and Bioenvironmental Sciences, Kyushu University, 6-10-1, Hakozaki, Higashi-ku, Fukuoka 812-8581, Japan
[b] Faculty of Agriculture, Tokyo University of Agriculture and Technology, 3-5-8 Saiwai-cho, Fuchu-shi, Tokyo 183-8509, Japan

ARTICLE INFO

Article history:
Received 10 October 2013
Received in revised form 9 March 2014
Accepted 22 May 2014
Available online 2 June 2014

Keywords:
Aqueous counter collision
Hierarchical structure
Nanofiber
Cellulose
Top-down process

ABSTRACT

This study involved a detailed investigation of a novel approach to reducing naturally occurring cellulose fibers into nanofibers solely by the use of aqueous counter collision (ACC) without any chemical modification. In this process, equivalent aqueous suspensions of cellulose are ejected from dual nozzles and collide at high speed and pressure. Even a few repetitions of the collision process are sufficient to produce nano-sized fibers dispersed in water. This work compared the ACC nano-pulverization of stable Iβ-rich and meta-stable Iα-rich cellulose samples. The ACC method is applicable to various kinds of polymeric materials with hierarchical structures, either natural or synthetic, as a means of preparing aqueous dispersions of nano-sized structures.

1. Introduction

Recently, we proposed a method of preparing separate cellulose nanofibers (so-called nanocellulose) as a dispersion in water, using aqueous counter collision (ACC) to process three-dimensional networks of fibers found in microbial cellulose pellicles. This technique allows bio-based materials to be processed into nano-objects using only a pair of water jets, without the need for any chemical modifications (Kondo et al., 2008; Kose, Mitani, Kasai, & Kondo, 2011). The nanocellulose obtained from the pellicle of the Gram-negative bacterium *Gluconacetobacter xylinus* (Kose et al., 2011) provided particular insight into the beneficial effects of using nano-sized materials by examination of its interactions with poly(lactic acid) (Kose & Kondo, 2013).

The ACC treatment of microbial cellulose was found to transform the cellulose Iα crystalline phase into a Iβ phase while maintaining its initial crystallinity. The transformation from Iα to Iβ was believed to occur on the nanofiber surfaces. It appears that the shear stress imparted by collisions with high speed water jets during the ACC treatment promotes the movement of cellulose molecules at the fiber surfaces required to rearrange the Iα phase to the Iβ phase. As the ACC treatment proceeds, therefore, the Iα phase at the fiber surfaces is transformed into the more stable Iβ phase, and this phase proceeds to cover the surface of the material. This newly generated Iβ surface was assumed to protect the nanocellulose from further transformation during subsequent exposure to the water jets (Kose et al., 2011).

In this article, we examine in detail the manner in which water jet energy and repeated collisions during the ACC process affect the nano-pulverization of micro-sized cellulose fibers. This study was performed using microcrystalline cellulose and the results are compared to data obtained using two naturally occurring nanocellulose materials: Iα-rich microbial cellulose from *Gluconacetobacter xylinus* and Iβ- rich animal cellulose from *Halocynthia*. This study had the additional aim of demonstrating that the ACC process has several advantages. The ACC method is easily able to provide nanofibers with desired widths, allowing the high volume production of high surface area fibers. In addition, without chemical surface modification, the surface properties and morphologies of the fibers can be tuned via the ACC treatment, for example to obtain superior adsorption of the fibers to various materials.

2. Materials and methods

2.1. Materials

Two samples of naturally occurring Iβ-rich cellulose materials were used: suspensions of microcrystalline cellulose crystallites (Funacel II®: Funakoshi Co., Ltd, Tokyo, Japan) and *Halocynthia* sp.

* Corresponding author. Tel.: +81 092 642 2997; fax: +81 092 642 2997.
E-mail addresses: tekondo@agr.kyushu-u.ac.jp (T. Kondo), biomaterial-design@hotmail.co.jp (H. Naito), wakako027@gmail.com (W. Kasai).

http://dx.doi.org/10.1016/j.carbpol.2014.05.064
0144-8617/

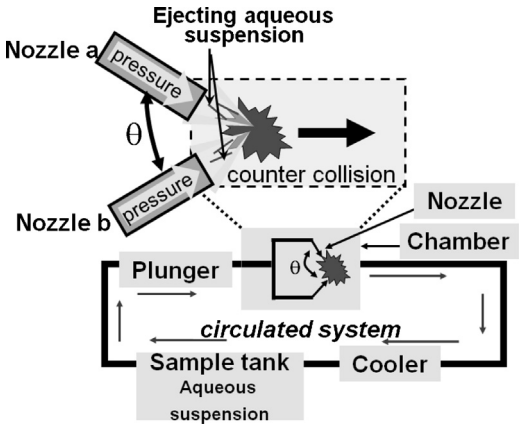

Scheme 1. The dual water jet aqueous counter collision (ACC) system.

The microcrystalline cellulose (Funacel II®) from wood pulp had a nominal degree of polymerization of 200–220 and a crystallinity index of 72%. A purified sample of the bleached tunic of *Halocynthia* sp. was treated with 100 mL of 65% sulfuric acid (w/w) at 70 °C for 30 h. The cellulose crystallites thus obtained then underwent successive washings with distilled water followed by centrifugation until the solution pH was in the range 1–5. The crystallinity index calculated from X-ray data obtained for the purified samples prior to acid hydrolysis was 86% (Hayashi, Sugiyama, Okano, & Ishihara, 1998) and the average crystallite size calculated from the (1–10) and (110) planes using Scherrer's equation (Patterson, 1939) was 8 by 9 nm.

Microbial cellulose secreted from *Gluconacetobacter xylinus* (formerly *Acetobacter xylinum*: ATCC53582) was employed as a naturally occurring source of Iα-rich cellulose crystallites, as detailed in our previous paper (Kose et al., 2011). The bacterium was inoculated into SH culture medium in a sterilized plastic container and cultured statically at 30 °C to yield a gel-like membrane having a 3D network structure formed from secreted cellulose nanofibers, known as a microbial cellulose pellicle. After 2 weeks of incubation, a pellicle approximately 1 cm thick was obtained, covering the top of the culture medium. The pellicle was removed and washed with 0.1% aqueous NaOH solution at 80 °C for 4 h and then washed successively with water over 3 days in order to remove protein, bacterial cells and other residues. The purified pellicle was cut into ca. 1 cm^3 cubes using scissors then immersed in deionized water. The crystallinity index of the cellulose in this material was found to be 84%.

To determine the I_α fraction in the whole cellulose crystalline phase, the characteristic CP/MAS ^{13}C NMR signals due to C1 carbons were deconvoluted by a Lorenzian curve fitting analysis (Kose et al., 2011). The resulting spectra exhibited one line assigned to I_α crystal lattice and two line assigned to I_β crystal lattice. The I_α fraction was calculated by the following expression:

I_α fraction/% = (areas of one line assigned to I_α crystalline phase/total areas of three lines) × 100

2.2. Preparation of cellulose nanofibers using ACC treatments

An aqueous counter collision system made by the Sugino Machine Co., Ltd. of Japan was employed for ACC treatments in this study. As shown in Scheme 1, two aqueous suspensions containing the micro-sized sample particles are expelled through dual nozzles, whereupon the two streams collide against one another under high pressure, resulting in rapid, wet pulverization which forms an aqueous dispersion of nano-sized objects (Kondo et al., 2008).

Ejecting a liquid suspension of the sample through the pair of nozzles (a and b in Scheme 1) under high pressures ranging from 70 to 270 MPa forms a pair of water jets. The diameter of each nozzle is in the range 100–200 μm and the angle of collision (θ) between the two jets is typically in the range 95°–178°. In this study, θ was set to approximately 170° (5° deviation from head-on collision for each nozzle: see Eq. (5)) and a nozzle diameter of 160 μm was employed. The number of ejection steps and the ejection pressure may be adjusted to subject the sample to the desired quantity of pulverizing cycles (or "passes"). The quantity of collisions and the collision pressure are the critical factors in tailoring the properties of the resulting nanofibers. The collision of the jets generates heat according to Eq. (1) (Tanaka, 2003).

$$\Delta T = 0.25P/C\,\rho \quad (1)$$

In Eq. (1), ΔT is the temperature increase in °C, P is the ejection pressure in MPa, C is the specific heat of water (1.0) in kcal kg^{-1} $°C^{-1}$ and ρ is the density of water (1.0×10^3) in kg m^{-3}. As an example, a temperature increase of 50 °C is associated with a pressure of 200 MPa. As a result of this heat generation, a cooling system based on a flow of water is required immediately after the collision zone of the two jets in the chamber (see Scheme 1).

Iβ-rich cellulose standards were prepared by suspending varying quantities of microcrystalline cellulose (Funacel II®) in deionized water to prepare 400 g dispersions with the concentrations shown in Table 1. These suspensions were then subjected to ACC treatment at 200 MPa, employing 10, 20, 30, 40, 60, 80 or 90 passes. The Iα and Iβ-rich samples obtained from bacterial and *Halocynthia* cellulose were processed using ACC at the same pressure of 200 MPa and using either 10, 30 or 60 passes, typically dispersing 10.0 g of the microcrystalline cellulose in 800 mL of water to produce 1.2% (w/w) suspensions. These aqueous suspensions were then transferred into the sample tank of the ACC apparatus and ejected through the pair of water jets, leading to collision of the resulting streams at the chosen pressure of 200 MPa. The pulverization process could potentially be repeated anywhere between 1 and 180 passes. After the desired number of collisions had occurred, an aliquot of the treated suspension was taken from the sample tank and various analyses were conducted, as described in the following section.

When preparing naturally occurring cellulose samples for ACC processing, those suspensions containing 0.05, 0.1 and 0.2% (w/w) cellulose fibers in water were pre-treated with a homogenizer (Physcotron NS-51, Microtec Co., Ltd.) at 20,000 rpm for several minutes to reduce the cellulose particles in size such that they were less than approximately 160 μm in width.

2.3. Microscopic observations

Those cellulose fiber samples which were several μm wide were observed under the crossed Nicols of a polarized microscope. Microscopic images were acquired with a 40×/0.75 PH 2 HCX PL Fluotar objective lens (Leica Microsystems Inc., Wetzlar, Germany) coupled with a 1.25× Optivar lens, using a Leica DMRE microscope with a Hamamatsu C5810 color chilled 3CCD camera (Hamamatsu Photonics Co. Ltd., Shizuoka, Japan). Using this equipment, digitized image frames were captured, saved and then processed via contrast enhancement, scale calibration, statistical size analysis and cross-sectional analysis using Image Pro Plus software v.4.1 (Media Cybernetics, Inc., MD, USA).

In each sample obtained at a given pass value, the width and length of more than 50 nanofibers were measured. To allow the measurement of single cellulose nanofibers in ACC-treated aqueous suspensions, the suspensions were first diluted to 1.0×10^{-3} wt%, following which an aliquot of each suspension was applied to a copper grid, air-dried and negatively stained using a 2% aqueous uranyl

Table 1
Properties of nanofibers obtained from microcrystalline cellulose by ACC processing.

Pulverizing cycles (pass)	Cellulose concentration (wt%)	Degree of polymerization ($\times 10^2$)	Average fiber length (μm)	Average fiber (width/nm)
0 (starting sample)	1	2.2	28	11×10^3
10	1	2.1	1.3 ± 0.9	20 ± 7
20	1	2.1	1.3 ± 0.9	17 ± 7
60	1	2.1	0.92 ± 0.56	15 ± 6
120	1	2.1	0.72 ± 0.36	14 ± 4
60	2	2.1	0.72 ± 0.49	16 ± 3
120	2	2.1	0.79 ± 0.55	14 ± 5

acetate solution. Following this pretreatment, nano-cellulose fibers were observed by transmission electron microscopy (TEM; JEM-1010, JEOL Ltd., Tokyo, Japan) at 5 μA and an accelerating voltage of 80 kV. The negatives of the acquired images were scanned and digitized as tif files at 8 bit radiometric resolution and then processed with Image Pro Plus software v.4.1 (Media Cybernetics, Inc., MD, USA) to ascertain the widths and lengths of the nanofibers, in the same manner as described above for microfibers.

2.4. FTIR and wide-angle X-ray diffraction (WAXD) measurements

A 2.0 mg portion of each microcrystalline cellulose sample was ground together with 200.0 mg of dry KBr powder to prepare transparent discs for analysis by Fourier transform infrared (FTIR) spectroscopy. In the case of the ACC-treated samples, the treated suspension was dropped on a silicon substrate before being dried under vacuum at 60 °C to prepare film specimens. FTIR spectra of the fiber samples thus prepared were acquired over the range 400–4000 cm^{-1}, using an FTIR-620 (JASCO International Co., Ltd., Tokyo, Japan) spectrophotometer with a TGS detector, employing 32 scans and 2 cm^{-1} resolution. The spectra were normalized to the height of the peak corresponding to the C—O stretching mode peak at 1162 cm^{-1} to allow direct comparisons.

To examine samples under conditions close to their in situ dispersion state, WAXD specimens were prepared by rapid freezing with liquid nitrogen and then dried using a critical point drying device. WAXD images were captured on flat film using Ni-filtered CuKα radiation produced by a Rigaku RINT-2500 HF X-ray generator (Rigaku Co. Tokyo, Japan) at 40 kV and 40 mA. WAXD intensity curves were measured in the transmission mode using a scintillation counter at 40 kV and 200 mA through the 2θ range 5–40° at a scan rate of 0.5°/min. To determine the crystallinity of samples, the WAXD curves were deconvoluted by curve fitting analysis using Gaussian functions (Chen, Stipanovic, Winter, Wilson, & Kim, 2007; Kataoka & Kondo, 1999).

2.5. Viscosity and viscoelastic measurements

The intrinsic viscosities [η] of various cellulose samples were measured in a copper ethylene diamine solution according to a method previously described in the literature of *TAPPI Standard* T230 su-66 (Vink, 1971). Based on the measured viscosity of each sample, its degree of polymerization was calculated according to Eq. (2), which describes the relationship between intrinsic viscosity and degree of polymerization.

$$[\eta] = 1.67 \times DP^{0.71} (DP \sim [\eta] \times 190) \quad (2)$$

Here 1.67 and 0.71 are values specific to a cellulose/copper ethylene diamine solution.

The rheological properties of the samples were measured using a rotational rheometer (CSL100, Carri-Med Ltd., Surrey, UK) with a cone-plate fixture and a plate diameter of 60 mm. The rheometer was designed to prevent evaporation of water from the test solutions during measurements and all tests were performed at 25 ± 0.1 °C. Dynamic viscoelastic measurements were performed at frequencies ranging from 0.1 to 100 rad/s at a dynamic strain amplitude (γ) of 0.03 (3%), a value at which all samples showed linear viscoelasticity. The cellulose concentration in all sample suspensions was 1.2% (w/w).

2.6. Determination of tentative kinetic parameters for enzymatic hydrolysis of nanofibers

Cellulose nanofibers for use as substrates were obtained from ACC treatments applying different pass numbers and were subsequently enzymatically treated. Aqueous solutions (0.4 ml) containing 0.2% (w/w) of crude cellulase (Meicelase; Meiji Seika Pharma, Co. Ltd., Tokyo, Japan; a crude cellulase originating from *Trichoderma viride*) were added to 10 mL aliquots of aqueous substrate dispersions of varying concentrations, and these reaction mixtures were incubated at 30 °C for periods ranging from 1 to 90 min. Following this incubation, mixtures were placed in a boiling water bath for 10 min to inactivate the enzyme. The supernatants were isolated by centrifugation at 20 kG for 5 min, following which the Somogyi–Nelson method (Hatanaka & Kobara, 1980) was used to determine the presence of reducing sugars. The initial rate of hydrolysis was determined by calculating the increase in the quantity of end groups in the substrates on the basis of the above Somogyi–Nelson measurements. For all substrates, the relationship between $1/v$ and $1/[S]$ exhibited approximate linearity when portrayed as Lineweaver–Burk plots, where v and S are the initial hydrolysis rate (or velocity) and the substrate concentration in wt%. Two kinetic parameters, the Michaelis constant (K_m) and the maximum velocity (V_{max}, mg L^{-1} min^{-1}), were calculated from the Michaelis–Menten equation.

3. Results and discussion

3.1. Nanofiber production from microcrystalline cellulose via ACC

Sedimentation was observed to rapidly take place when the Iβ-rich microcrystalline cellulose was initially dispersed in water. These suspensions were nonetheless subjected to ACC processing. Following five replicate ACC treatments (equivalent to five passes), the sedimentation seen in the initial sample was no longer present. Instead, a white, turbid suspension was obtained which was stable on standing for periods of at least 24 months. This stability is presumably due to the formation of micelles, since the sub-fibrillated fibers resulting from the ACC process are approximately 20 nm wide and are capable of binding water. The TEM images in Fig. 1 also show nano-fibrillation at the end of the microfiber, indicating that the ACC treatment peels off nanofibers 15–20 nm in width from the sample surface to produce the resulting aqueous suspension.

Further treatment using over 20 passes provided a translucent aqueous dispersion with higher viscosity. As shown in Table 1, nanofibers 15–20 nm in width and 1 μm in length were obtained from the ACC process. The average length of these nanofibers was

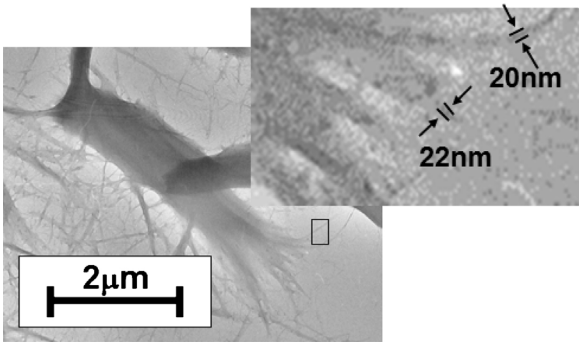

Fig. 1. TEM images of a sample following five passes through the ACC process. The upper inset indicates the enlarged TEM image of the rectangle part.

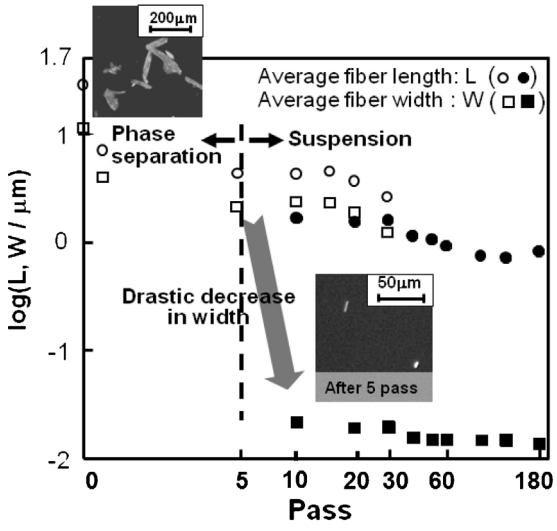

Fig. 2. Change in the length (L) and width (W) of cellulose fibers with repeated passes through the ACC process. The filled symbols indicate data from TEM observations, whereas the unfilled symbols are based on polarized microscopy. The inserts show polarized micrographs of suspensions prior to treatment and after five passes. Before five pass, the solid square points were overlapped with empty square points.

still longer than the molecular chain length determined by viscometry, suggesting that the nanofibers contained at least some crystalline domains even after 120 passes through the ACC treatment.

The nano-pulverization of the cellulose microfibers during ACC was monitored by examining changes in the fiber sizes using a polarized microscope under crossed-Nicols, and by TEM (see Fig. 2). Up to 30 passes, the polarized microscope was mainly employed to observe the initial stages of the ACC pulverization of the starting microfibers. These observations showed that, with increasing passes, the average fiber length was not greatly decreased. In contrast, the fiber widths were drastically decreased after the initial phase separation was observed to disappear at five passes, even though some micro-sized fibers still remained (see the inset of the polarized micrograph in Fig. 2). Thus nano- and microfibers co-exist in the dispersion between five and 30 passes (as shown in the figure, in which both filled and empty symbols coexist at the same pass values). Above 30 passes, the microfibers are no longer observed, indicating that the majority of these microfibers have transitioned into nanofibers dispersed in water at this point.

As noted above, during the ACC process, both micro- and nano-sized cellulose fibers coexist in the suspension at some points. Thus changes in the ratio of micro- to nano-sized fibers were monitored based on data obtained by centrifugal precipitation. According to the Stokes equation for sedimentation under gravitational force (Eq. (3)), colloidal spheres of radius a will precipitate as follows (van Holde, Johnson, & Ho, 1998).

$$V/T = 2a^2(\rho_p - \rho_m)g/9\eta \quad (3)$$

Here V is the sedimentation volume in cm^3, T is the sedimentation time in s, ρ_p is the density of the colloidal spheres, ρ_m is 1 g cm^{-3} (the density of water), g is acceleration due to gravity and η is 1 mPa s (the viscosity of water). The short microcrystalline cellulose fibers employed in this study were assumed to be colloidal spheres in the ACC-treated suspensions and the density of the cellulose crystals was given a value of 1.6 g cm^{-3}.

During centrifugation of ACC-treated suspensions for 10 min at 0.37 kG, it was assumed that only spheres greater than 1.1 μm in diameter would precipitate, according to Eq. (3) when L = 9 cm was employed as the length of the centrifuge tube. As such, only nano-objects were considered to be present in the supernatant, resulting in selective separation of the cellulose nanofibers from the treated suspensions. As shown in Table 1, the nanofibers obtained under various ACC conditions exhibit average widths in the range 10–20 nm and are about 1 μm in length. Prior to the ACC treatment, 100% of the cellulose can be precipitated. As the ACC treatment is repeated up to 40 passes, the proportion of microcellulose decreases to a few percent, indicating almost complete nano-pulverization by the water jets at a pressure of 200 MPa. As shown in Table 1, ten passes are, on average, sufficient to produce cellulose nanofibers from the starting microfibers. The size of the nanocellulose fibers eventually plateaus at 14 ± 4 nm at a pressure of 200 MPa. As will be reported in a future publication, the ejection pressure, rather than the number of passes, is actually more effective in terms of improving the efficiency of pulverization, such that higher water jet speeds generate smaller fiber sizes. Furthermore, the initial sample concentration (within the range 1–2%) does not significantly influence the nano-pulverizing effect during ACC treatment (see the data below the line in Table 1).

Transparent films of the cellulose nanofibers were obtained simply by casting the individual ACC-treated suspensions. This is in contrast to the turbid nature of the starting suspensions. This transparency indicates that the fibers have widths below the optical wavelength of light (see Table 1).

3.2. Characterization of nanofibers obtained by ACC treatments of microcrystalline cellulose

From analysis of the IR spectra of the above-noted transparent cast films of sample suspensions, it was confirmed that these spectra were identical to the spectrum of the initial microcrystalline cellulose, even after 180 passes. The IR spectrum of the precipitated microcellulose obtained from centrifugation was also identical to that of the nanocellulose in the supernatant. As shown in Table 1, there was no evidence that either depolymerization or hydrolysis occurred as a result of the ACC treatment and thus this process does not modify the materials at the molecular level.

Regardless of the number of passes, wide angle X-ray diffraction (WAXD) measurements obtained from samples after rapid freezing showed that the majority of the cellulose in the suspensions exhibited a diffraction pattern identical to that of the monoclinic crystalline lattice of native cellulose Iβ, which is completely different from the WAXD pattern of the regenerated cellulose II form (data not shown). This result, together with the TEM images in Fig. 1, indicates that ACC treatment does not necessarily allow the samples to dissolve in water, but rather produces a dispersion of crystalline nanofibers. The width and length of the crystalline

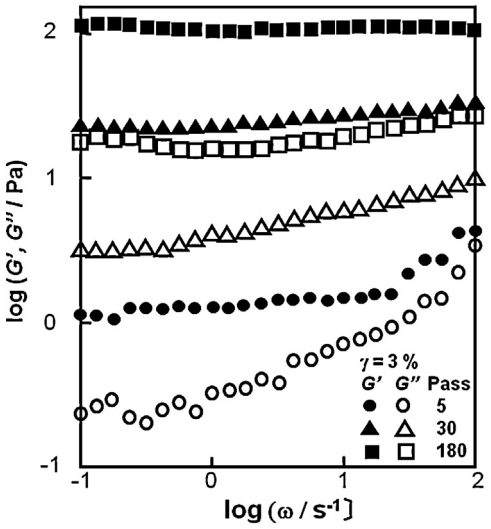

Fig. 3. Dynamic storage modulus, G', and loss modulus, G'', as functions of angular frequency, ω, for 5, 30 and 180 passes through the ACC process. Samples had a cellulose concentration of 1.2%, w/w.

domains were roughly estimated by applying the Scherrer equation (Patterson, 1939) (Eq. (4)) to the diffraction intensity curves of the (2 0 0) and (0 0 4) planes.

$$D = 0.9\lambda/\beta_{1/3} \cdot \cos\theta \quad (4)$$

In Eq. (4), D is the estimated size of the crystalline domain, λ is the X-ray wavelength and $\beta_{1/2}$ is the half-width of the reflection intensity curve. Although the degree of crystallinity plateaus at 50% after 30 passes, the widths of the crystalline domains continue to decrease up until 90 passes (data not shown). This tendency indicates that the generation of nanofibers during ACC treatment occurs at the surfaces of the microcrystalline cellulose fibers as they are systematically broken down into single nanofibers. Further treatment beyond 90 passes increases the fiber width, and this may indicate re-aggregation of the crystalline nanofibers. However, analyses on rheological properties of nanocellulose dispersions, as described in the following, demonstrated that the suspension was fairly stable after 2 h following ACC treatment, because three-dimensional aggregates might have already been formed. In the present case, re-aggregation also occurred possibly during drying for the sample preparation. Conversely, there was no significant change during ACC treatment in the lengths of the crystalline domains based on measurements of the (0 0 4) plane.

3.3. Rheological properties of nanocellulose dispersions in water after ACC treatments

Fig. 3 presents the frequency dependence of the dynamic storage modulus, G', and the loss modulus, G'', of aqueous dispersions obtained by ACC treatments of microcrystalline cellulose, applying various numbers of passes. Both moduli are almost constant, independent of the angular frequency, ω, in the case of the aqueous dispersions obtained after more than 30 passes. G' is seen to be approximately ten times larger than G'' at all the applied frequencies. This indicates that these systems behave predominantly as elastic materials (Onogi, Masuda, & Matsumoto, 1970) and also suggests that three-dimensional aggregates might be formed by entanglements between the cellulose nanofibers.

There are no significant differences in the G' values of solutions produced using the same number of passes as they stand for periods between 2 and 7 h following ACC treatment. Therefore the suspensions, once they are prepared, appear to be fairly stable after 2 h following ACC treatment without any tendency toward further self-aggregation. As the pass number is increased from 5 to 180, G' increases monotonically, possibly due to increased pulverization leading to stronger interactions between fibers (Lewis & Nielsen, 1970). The rheological properties of aqueous dispersions prepared under various ACC conditions and a variety of different pre-treatments are still under investigation, and will be reported in a future paper.

Table 2
Relationship between water ejection pressure and calculated kinetic energy of water molecules, in addition to a summary of bond energies.

Ejecting pressure (MPa)	Kinetic energy (kJ mol^{-1})
50	3.6
100	7.2
150	10.8
200	14.3
Type of bond	**Bonding energy (kJ mol^{-1})**
H—OH (covalent bond)	499
H—H (covalent bond)	436
Ion–ion	250
Medium hydrogen bond	21–62
Weak hydrogen bond	4.2×10^{-1}–4.2
London dispersion force	2
Dipole–dipole	0.6–2

3.4. Collision and intercalation of high speed water jets during ACC treatments

The nano-pulverization effect of the ACC process may be considered simply as a direct consequence of the force of the collision between the paired water jets and the subsequent intercalation of water into hierarchical structures of the sample fibers. The kinetic energy imparted by the jets of water molecule/mol was approximately estimated in the system using following Eq. (5):

$$K = \frac{mv_x^2}{2}, \quad v_x = v \times \cos(5^\circ), \quad v = C_v\left(\frac{2P \times 10^3}{\rho}\right)^{1/2} \ldots \quad (5)$$

where K: kinetic energy in kJ mol^{-1}, m: weight of the water molecule in kg mol^{-1}, v_x: velocity in m·s^{-1}, v: initial velocity when ejected in m s^{-1}, ρ: density of water ($\approx$1) in g cm^{-3}, P: ejecting pressure in MPa, and C_V: velocity constant ($\approx$1) dimensionless.

In our study, four different ejection pressures were employed, as shown in Table 2. The kinetic energies associated with each were calculated using the aforementioned equations and are provided in the same table. A single ACC pass can evidently impart kinetic energy between 6.7 and 18.1 kJ/mol, which is more than the energies associated with dipole–dipole, London dispersion forces and weak hydrogen bonds (see the bottom section of Table 2) (Jeffrey & Saenger, 1991). Based on these values, it should be possible to effectively reduce the particle sizes of various polymeric materials with hierarchical structures, either natural or synthetic, using ACC treatment. As an example, the jet pressure of 200 MPa that is normally used in this process can provide energy more than sufficient to break weak or medium strength hydrogen bonds. In the present study, the resulting nanofibers which are approximately 15 nm in width (see Table 1) are believed to involve relatively strong hydrogen bonding between molecules and hence remain intact during the ACC treatment.

3.5. Iα-rich microbial cellulose from Gluconacetobacter xylinus vs. Iβ-rich animal cellulose from Halocynthia

Naturally occurring cellulose I crystals are a composite of two distinct crystalline forms: triclinic Iα and monoclinic Iβ phases

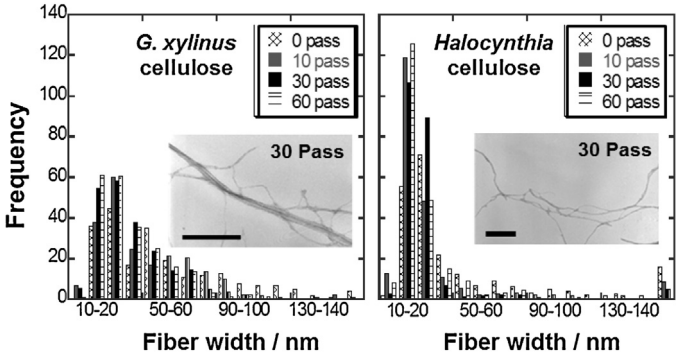

Fig. 4. Comparison of the width distributions of cellulose nanofibers from *G. xylinus* and *Halocynthia* cellulose, following ACC treatments involving 0, 10, 30 and 60 passes. The insets show TEM images acquired after 30 passes. Both scale bars indicate 500 nm.

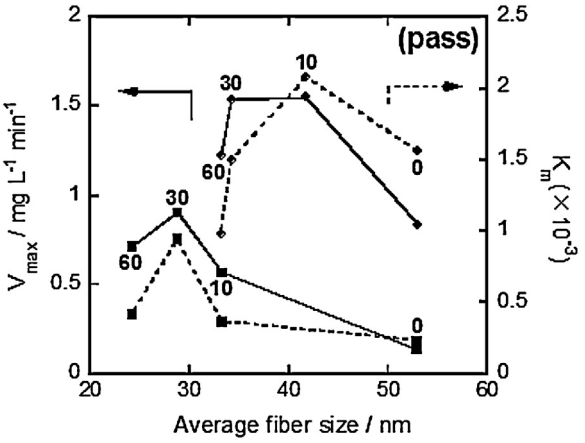

Fig. 5. Relationship of the Michaelis constant (K_m) and the maximum velocity (V_{max}) with the average fiber width of cellulose nanofibers prepared by ACC. The full and dotted lines indicate changes in V_{max} and K_m, respectively. Legend: ● = *G. xylinus* cellulose, ■ = *Halocynthia* cellulose.

(Atalla & Vander Hart, 1984). Microbial cellulose from *Gluconacetobacter xylinus* is Iα-rich, whereas animal cellulose from *Halocynthia* is primarily composed of Iβ· In a previous paper (Kose et al., 2011), we reported that single cellulose nanofibers ("nanocellulose") obtained from microbial cellulose pellicles using ACC forms three dimensional networks when dispersed in water. The ACC treatment also transforms the Iα crystalline phase into the Iβ phase while maintaining the initial degree of crystallinity. In the present study, animal cellulose (Iβ-rich) from *Halocynthia* was subjected to ACC processing at 200 MPa and the obtained nanofibers were compared with the results formerly obtained when processing microbial cellulose (Iα-rich) from *Gluconacetobacter xylinus.* Fig. 4 compares the width distributions of cellulose nanofibers obtained from ACC processing of *G. xylinus* and *Halocynthia* celluloses. The nanofibers from the *Halocynthia* cellulose rapidly plateau at sizes within the range 20–30 nm in width, whereas nanofibers obtained from microbial cellulose have a much wider size distribution, as reported previously (Kose et al., 2011).

This difference is also confirmed by the inset TEM images in Fig. 4, which show that *G. xylinus* cellulose was nano-fibrillated (Kose et al., 2011) while *Halocynthia* cellulose was converted into homogeneous nanofibers. Moreover, the narrower size distribution of the Iβ-nanofibers also indicates that the Iβ-rich *Halocynthia* cellulose is more stable during the ACC treatment. As reported in a previous study (Kose et al., 2011) on the transformation of the Iα crystalline phase into the Iβ phase by the ACC method, the branched subfibrils and the newly exposed nanofiber surfaces may be covered with stable Iβ-rich crystalline phases, resulting in some resistance to further nano-pulverization.

The two kinds of nanofibers were also subjected to enzymatic hydrolysis with crude cellulase from *T. viride* to allow an estimation of their respective enzymatic stabilities. As shown in Fig. 5, the Iα-rich microbial cellulose nanofibers are more readily hydrolyzed compared with the Iβ-rich *Halocynthia* cellulose nanofibers (Hayashi et al., 1998). In both cases, the samples exhibit a maximum value of V_{max} after 30 passes, resulting in widths of approximately 34 and 29 nm for the microbial and *Halocynthia* nanofibers, respectively. Both specimens also show reduced V_{max} values at 60 passes. One reason for this phenomenon in the case of the microbial cellulose nanofibers could be coverage of the surfaces with stable Iβ-rich crystalline phases due to complete crystalline transformation at 60 passes. Another explanation, which is applicable to both nanofibers, is that the fiber widths are more homogeneously distributed after 60 passes and therefore self-aggregation of the nanofibers becomes important. This in turn decreases the surface area available for adsorption of the carbohydrate-binding modules (CBMs) in the cellulase. The observed decrease in both Km values at 60 passes indicates an increase in the adsorption process between the substrates and the cellulase, which induces some extra-adsorption of CBMs to the substrates, leading to a reduction in V_{max}. It is noteworthy that the Km values of the Iβ-rich *Halocynthia* cellulose are uniformly lower than those of the microbial cellulose. These results agree with the outcome of a previous study that found the maximum adsorption of the enzyme onto cellulose Iβ was higher than the maximum rate of adsorption onto cellulose Iα, although the rate of cellobiose production from cellulose Iβ was lower than that from cellulose Iα (Igarashi, Wada, Hori, & Samejima, 2006). In the present case, the maximum adsorption of the enzyme onto cellulose Iβ was significantly higher than the adsorption onto the Iα phase, in excess of the ratio of 1.5 which has been previously reported. This is due to the so-called nano-size effect.

With regard to the action of CBMs, tryptophan residues in the subsites are reported to mediate the interaction of the cellulase with cellulose (Rouvinen, Bergfors, Teeri, Knowles, & Jones, 1990) and so the hydrophobicity of the amino acid residues involved in cellulase–substrate interactions cannot be disregarded. It will therefore be necessary to investigate the effects of the increased hydrophobicity of nanofiber substrates prepared by the ACC method to better predict cellulase–substrate interactions.

4. Conclusions

This study represents a detailed investigation of the aqueous counter collision technique as a rapid nano-decomposition process capable of preparing cellulose nanofibers from microcrystalline wood cellulose. Our work has also applied ACC to microbial and animal celluloses and compared the resulting nanofibers to one another with regard to their chemistry, morphology and basic rheology. Rough estimates of the enzymatic hydrolysis rates of the various nanofiber aqueous dispersions were also obtained.

During preparation of these nanofibers, it is possible to control the fiber widths such that specific surface properties may be obtained, although this effect varies with the fiber structure and surface morphology. Based on our results, a more thorough understanding of the relationship between the fiber structures and their properties could be the key to finding future applications of this process. Using the ACC nanofiber preparation method, various nano-size effects could also be examined in various materials.

The advantages of this ACC method may be summarized as: (i) it is a rapid, means of processing cellulose into nanofibers using only

water and without chemical modification, (ii) it is applicable not only to cellulose but also to other polymeric materials having hierarchical structures. Moreover, the obtained aqueous dispersions of nanocellulose materials are fairly stable for at least several hours because of formation of three dimensional aggregation soon after ACC treatment, in the sense that significant further self-aggregation does not appear to take place. Therefore this process represents a helpful tool for the future detailed study of nano-sized structures and their applications.

Acknowledgements

We would like to thank Mr. Eiji Togawa at the Forestry and Forest Products Research Institute (FFPRI), Tsukuba, Japan for kindly assisting in this work by performing the wide angle X-ray diffraction analyses. The authors are also indebted to Prof. Akihiko Takada at the Institute for Materials Chemistry and Engineering, Kyushu University, Japan for his valuable comments.

References

Atalla, R. H., & Vander Hart, D. L. (1984). Native cellulose. A composite of two distinct crystalline forms. *Science*, *223*, 283–285.

Chen, Y., Stipanovic, A. J., Winter, W. T., Wilson, D. B., & Kim, Y.-J. (2007). Effect of digestion by pure cellulases on crystallinity and average chain length for bacterial and microcrystalline celluloses. *Cellulose*, *14*, 283–293.

Hatanaka, C., & Kobara, Y. (1980). Agricultural and biological chemistry determination of glucose by a modification of Somogyi–Nelson method. *Agricultural and Biological Chemistry*, *44*, 2943–2949.

Hayashi, N., Sugiyama, J., Okano, T., & Ishihara, M. (1998). Selective degradation of the cellulose Iα component in Cladophora cellulose with Trichoderma viride cellulose. *Carbohydrate Research*, *305*, 109–116.

Igarashi, K., Wada, M., Hori, R., & Samejima, M. (2006). Surface density of cellobiohydrolase on crystalline celluloses A critical parameter to evaluate enzymatic kinetics at a solid–liquid interface. *FEBS Journal*, *273*, 2678–2869.

Jeffrey, G. A., & Saenger, W. (1991). *Hydrogen bonding in biological structures*. Berlin, Germany: Springer-Verlag.

Kataoka, Y., & Kondo, T. (1999). Quantitative analysis for the cellulose Iα crystalline phase in developing wood cell walls. *International Journal of Biological Macromolecules*, *24*, 37–41.

Kondo, T., Morita, M., Hayakawa, K., & Onda, Y. (2008). Wet pulverizing of polysaccharides. U.S. Patent 7,357,339.

Kose, R., Mitani, I., Kasai, W., & Kondo, T. (2011). "Nanocellulose" as a single nanofiber prepared from pellicle secreted by *Gluconacetobacter xylinus* using aqueous counter collision. *Biomacromolecules*, *12*, 716–720.

Kose, R., & Kondo, T. (2013). Size effects of cellulose nanofibers for enhancing the crystallization of poly(lactic acid). *Journal of Applied Polymer Science*, *128*(2), 1200–1205.

Lewis, T. B., & Nielsen, L. E. (1970). Dynamic mechanical properties of particulate-filled composites. *Journal of Applied Polymer Science*, *14*, 1449–1471.

Onogi, S., Masuda, T., & Matsumoto, T. (1970). Non-linear behavior of viscoelastic materials I. Disperse systems of polystyrene solution and carbon black. *Transactions of the Society of Rheology*, *14*(2), 275–294.

Patterson, A. L. (1939). The Scherrer formula for X-ray particle size determination. *Physical Review*, *56*, 978–982.

Rouvinen, J., Bergfors, T., Teeri, T., Knowles, J. K. C., & Jones, T. A. (1990). Three-dimensional structure of cellobiohydrolase II from *Trichoderma reesei*. *Science*, *249*, 380–386.

Tanaka, K. (2003). Techincal review of the "Ultimizer system". *Sentankakou (in Japanese)*, *21*, 15–19.

TAPPI Standard T230 su-66. (Standard of The United States Association of Paper and Pulp Industry) employing cupri-ethylenediamine as a solvent. A higher viscosity of pulp means a greater strength of cellulose.

van Holde, K. E., Johnson, W. C., & Ho, P. S. (1998). *Principles of physical biochemistry*. Upper Saddle River, NJ: Prentice-Hall, Inc.

Vink, H. (1971). In N. M. Bikales, & L. Segal (Eds.), *Cellulose and cellulose derivatives part IV* (pp. 469–489). New York, NY: John Wiley & Sons, Inc.